

Design of a Real-Time Indoor Positioning System Based on Visible Light Communication

Marcos S. P. dos S. LIMA JUNIOR¹, Miklos Peter HALAPI², Eszter UDVARY³

¹ Furukawa Electric LatAm, Rua Hasdrubal Bellegard, 820 - ZIP 81460-120, Curitiba-PR, Brazil

² Furukawa Electric Institute of Technology, Kesmark u. 28/A, H-1158 Budapest, Hungary

³ Dept. of Broadband Info-Communication and Electromagnetic Theory, Budapest University of Technology and Economics, 3 Muegyetem rakpart, 1111 Budapest, Hungary

{marcos.pacheco, miklos.halapi}@furukawaelectric.com, udvary@hvt.bme.hu

Submitted December 15, 2019 / Accepted June 22, 2020

Abstract. *In this paper a real-time Indoor Positioning System (IPS) based on Visible Light Communication (VLC) is proposed, deployed and studied. It is composed of nine LED-based VLC transmitters installed in the ceiling of an indoor environment, each of them transmitting different ID codes that are detected by a photodiode-based mobile correlator receiver. The receiver is able to measure the distance between itself and the transmitters and use this information to estimate its own position in the environment. The distances are measured using Received Signal Strength (RSS), where initial experiments were executed in order to determine physical parameters of the system. Then, the 2D or 3D position is estimated by the receiver using multilateration in real-time. This paper also brings tests and discussions regarding the accuracy achieved by the deployed system.*

Keywords

Indoor Positioning Systems (IPS), Visible Light Communications (VLC), Received Signal Strength (RSS), multilateration

1. Introduction

The current outdoor positioning systems, such as Global Positioning System (GPS) and Global Navigation Satellite System (GLONASS) are widely available in many devices in the market since the 90's, and it has brought the possibility to know our location and the location of any devices around the world [1]. It is difficult to imagine our lives without the benefits of this technology when tracing routes throughout the streets and roads, for example.

However, considering the positioning inside public or private places, it is not possible to visualize the same scenario. For instance, inside buildings, metro stations, factories, sheds, and other sites GPS and other satellite-based positioning systems do not have the same accuracy as outside, or they do not work with the same reliability, some-

times reaching an error of several dozens of meters [2]. On the other hand, in indoor environments, some positioning methods exist, but these technologies are not so popular and/or are limited by accuracy, complexity, cost, power consumption, range, robustness and scalability [3]–[6].

This is the reason why Visible Light Communication prospects a promising solution for indoor localization systems, where the same source of light might be used for illumination, communication and positioning through the modulation of commercially available light-emitting diodes (LEDs) [7]. These advantages are reinforced by the fact that such systems can achieve high bandwidth, low latency, and high positioning accuracy using license-free spectrum immune to electromagnetic interferences [8], [9].

In addition to these advantages, the wide variety of different approaches of modulation, multiplexing, sensing, demodulation, position estimation, tracking and localization strategies proposed by several authors motivates this study. It leads to an extensive number of different technology combinations to be studied in order to find results with promising accuracy, reliability, and scalability [3], [10]–[13], [16].

In this sense, the present work deals with the practical results of a real-time IPS deployed in an office environment using nine VLC-based transmitters and one photodiode-based receiver. The goal of this system is to combine several techniques such as: On-Off Keying (OOK) Non-Return to Zero (NRZ) modulation with low cross-correlation preambles, Time Division Multiplexing (TDM), Received Signal Strength (RSS), correction of the light fixtures' directivity and a dynamic technique of multilateration for achieving a good performance real-time indoor positioning system.

This article is organized as follows: Section 2 does an overview of the design of the IPS; Section 3 describes the positioning algorithm deployed; Section 4 presents the results achieved by the proposed positioning system; Section 5 discusses the results presented by Section 4; and Section 6 brings a conclusion of the work presented in this paper.

2. Description of the System

The prototype of the VLC IPS was realized in a room with $8\text{ m} \times 3.8\text{ m} \times 2.6\text{ m}$ in which 20 light fixtures were evenly installed so that 9 of them were connected to transmitters, while the 11 remaining were connected to current-controlled power supplies as it is shown in Fig. 1 and Fig. 2.

The arrangement of the 9 transmitters allowed the estimation of the mobile receiver’s position using multilateration in the majority of the room area and also contributed to a better understanding of the effect of the reflections coming from the walls in the position accuracy. In addition, the remaining 11 light fixtures guaranteed an even illuminance in the entire room area.

All transmitter boards were connected through RS-485 to an interface board responsible for scheduling the TDM communication, and each one of them received a different identification code so that only one transmitter modulates its own code at a time. The modulation and control of transmitter functions were coordinated by a microcontroller unit (MCU).

In the receiver, a photodiode-based circuit with a transimpedance amplifier was responsible for transforming the light signals into voltage levels in a printed circuit board (PCB) designed specifically for this purpose. As shown in Fig. 3, this board was connected to a mini computer in which a decoding process was performed using a correlator

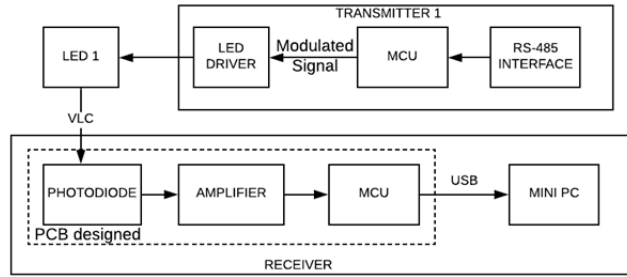


Fig. 3. VLC IPS block diagram: the connection between one transmitter and the receiver and their sub-components.

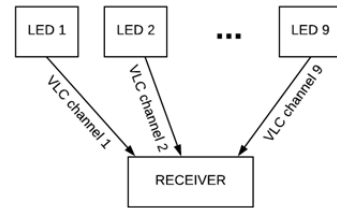


Fig. 4. Unidirectional VLC optical channels.

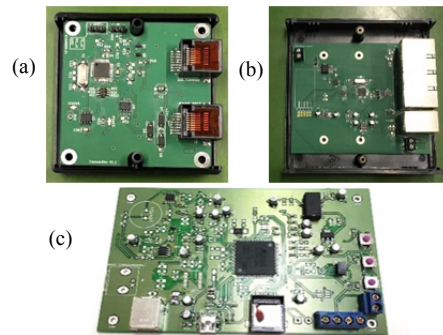


Fig. 5. VLC IPS hardware: (a) transmitter; (b) interface board; (c) receiver (designed PCB).

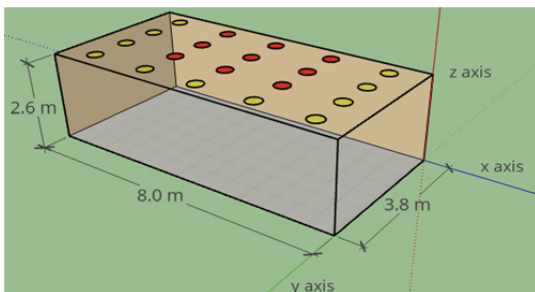


Fig. 1. Distribution of the light fixtures in the room: connected to transmitters (red) and connected to standard power supplies (yellow).



Fig. 2. Light fixtures connected to transmitters after installation.

receiver so that it was possible to identify from which light fixtures the signals were coming. The mini-computer was also responsible for the RSS calculations and for performing real-time positioning algorithms.

It is important to point out that the transmission is unidirectional from transmitter to receiver, as it is shown by Fig. 4. This way, no acknowledgement or retransmission of a single ID message is possible. Thus, if any of the signals received from the transmitters was identified as erroneous or corrupted it was dropped in order to have real-time position estimations.

The final design of the VLC IPS hardware, consisting of transmitter, interface and receiver printed circuit boards is shown in Fig. 5.

3. Positioning Algorithm

3.1 Distance Estimation

First, the distance between the LEDs and the receiver was calculated using RSS [14]:

$$d = \sqrt{\frac{P_r}{P_t} R_t(\varphi) A_{\text{eff}}(\psi)} \quad (1)$$

where P_r is received power, P_t is transmitted power, d is the distance between transmitter and receiver, $R_t(\varphi)$ is the transmitter radiant intensity which depends on the radiation angle (φ) and $A_{\text{eff}}(\psi)$ is the effective signal receiving area that is a function of the receiving angle (ψ).

As the photodiode utilized had a built-in lens with the purpose of maximizing A_{eff} for a wide receiving angle range, it was considered as a constant k_A for any receiving angle.

On the other hand, it was not possible to use the same consideration for $R_t(\varphi)$ because φ presents a strong influence in the transmitter radiant intensity for the proposed system depending on the Lambertian order m , as follows [14]:

$$R_t(\varphi) \propto \cos^m \varphi \quad (2)$$

where the Lambertian order is defined by (3) using the half-power angle $\varphi_{1/2}$ [14]:

$$m = -\frac{\ln 2}{\ln(\cos \varphi_{1/2})} \quad (3)$$

In the particular case of this work, the half-power angle is approximately 45° as shown in Fig. 6, and the light fixtures were considered as a second order Lambertian radiator ($m = 2$) for any direction within a plane parallel to its diffuser. Thus, if $R_t(\varphi)$ was considered as a constant, it would lead to a compromised accuracy in the positioning system due to erroneous distance measurements, and for this reason the effect of φ in the distance measurement had to be considered.

Following those propositions, it was possible to rewrite the RSS distance equation:

$$d = \sqrt{\frac{P_t}{k_1 V_m} k_A k_R \cos^2 \varphi} \quad (4)$$

where V_m is the voltage measured by the receiver which is proportional to the light power sensed and the constants k_1 , k_A and k_R are related respectively to the receiver conversion gain from optical power to voltage, to the effective signal receiving area of the photodiode and to the transmitter radiant intensity.

Finally, as P_t is also a constant value because the power transmitted is considered to be always the same, the distance can be fitted in terms of V_m resulting in a numerical equation that can be used for multilateration:

$$d = \sqrt{\frac{1}{C \cdot V_m}} \cos \varphi \quad (5)$$

where C was estimated in the experiment presented in Fig. 7, in which the goal was to measure the value of V_m at several distance values (d) with $\varphi = 0^\circ$ so that the curve fitting shown in Fig. 8 could be accomplished.

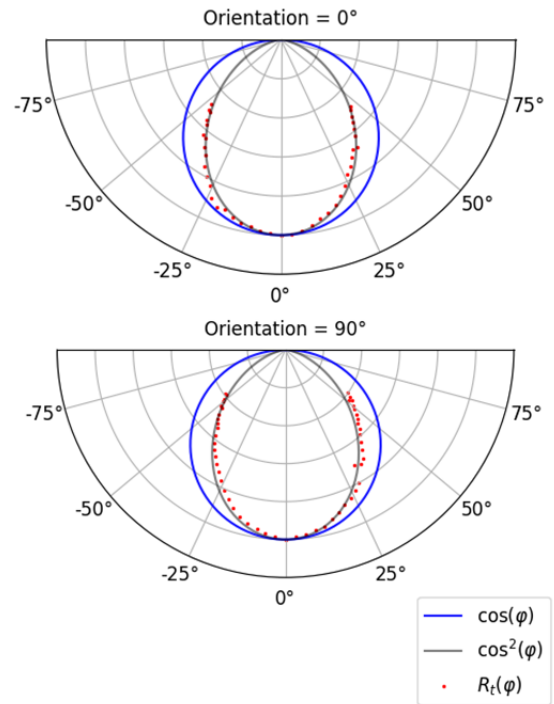


Fig. 6. Measured directivity of the light fixtures (in terms of normalized $R_t(\varphi)$) with orientation $\varphi = 0^\circ$ (top) and $\varphi = 90^\circ$ (bottom) within the plane parallel to the light fixture diffuser.



Fig. 7. Setup assembled for the estimation of C .

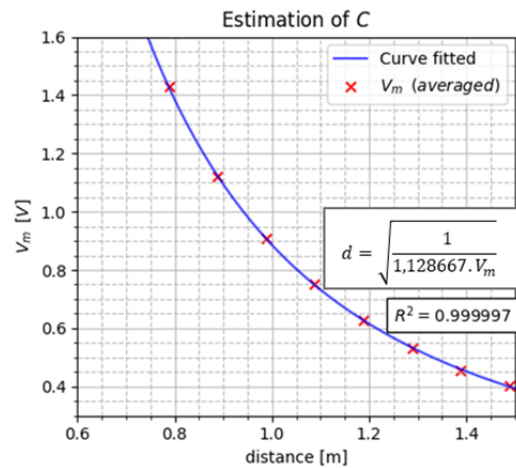


Fig. 8. Plot of d versus V_m and curve fitting.

3.2 Position Estimation with Multilateration

This work used multilateration for estimating the 3D position of the mobile device inside the room. This method consists in defining a set of equations based on Euclidian distances which can be solved by using numerical approaches [1]. The system of equations for a multilateration problem can be defined by (6).

$$(x - x_i)^2 + (y - y_i)^2 + (z - z_i)^2 - d_i^2 = e_i; \quad (6)$$

$$i = 0, \dots, N-1; N \geq 4$$

where (x, y, z) coordinate represents the unknown position, (x_i, y_i, z_i) represents the coordinate of the i^{th} light fixture, d_i the Euclidian distance between the i^{th} light fixture and the mobile receiver and e_i is the error to be minimized by the numerical solver algorithm of the system of equations.

In order to keep only 3 unknowns (x , y and z) in the system of equations, the distance equation presented in the previous sub-section can be rewritten in terms of $(z_i - z)$, as $\cos \varphi_i = (z_i - z)/d_i$:

$$d_i^2 = \sqrt{\frac{1}{C \cdot V_{m_i}}} (z_i - z), \quad (7)$$

and the estimated 3D coordinate \hat{p} could be found with N as the maximum number of reliable transmitters detected in each cycle of measurements, using the following equations:

$$\begin{cases} (x - x_0)^2 + (y - y_0)^2 + (z - z_0)^2 - \sqrt{\frac{1}{C \cdot V_{m_0}}} (z_0 - z) = e_0, \\ (x - x_1)^2 + (y - y_1)^2 + (z - z_1)^2 - \sqrt{\frac{1}{C \cdot V_{m_1}}} (z_1 - z) = e_1, \\ \vdots \\ (x - x_{N-1})^2 + (y - y_{N-1})^2 + (z - z_{N-1})^2 - \sqrt{\frac{1}{C \cdot V_{m_{N-1}}}} (z_{N-1} - z) = e_{N-1}, \end{cases} \quad (8)$$

$$\hat{p} = \arg \min_{x, y, z} \sum_{i=0}^{N-1} e_i. \quad (9)$$

4. Results

In order to check the effectiveness of the VLC IPS designed, the mobile receiver was placed in several points inside the room and its position was estimated by software in the mini-computer using the procedure described by Sec. 3.2. As the receiver could not detect all the transmitters in every position of the room due to limitations in the amplification range of the receiver, the multilateration was performed with the maximum number of transmitters detected for each point. This value for each position was stored for further investigations.

Then, the position estimate for every measurement was compared to the real position of the receiver in the room (measured with a measuring tape with tolerance ± 0.6 mm), so that the positioning error could be calculated. This process was repeated three times and averaged for every location p in each 50 cm of $0 \leq x \leq 4$ m and $0 \leq y \leq 3.8$ m axes of the semi-plane P with $z = 0.85$ m:

$$\frac{1}{3} \sum_{i=1}^3 (\hat{x}_i - x_{\text{real}})^2 + (\hat{y}_i - y_{\text{real}})^2 + (\hat{z}_i - z_{\text{real}})^2 = 3D \text{ error}_p, \quad (10)$$

$$\frac{1}{3} \sum_{i=1}^3 (\hat{x}_i - x_{\text{real}})^2 + (\hat{y}_i - y_{\text{real}})^2 = 2D \text{ error}_p. \quad (11)$$

As described, the measurements were conducted in half of the room's area as the dimension of the room in axis x is 8 m. Thus, it is expected that the other half of the room (for $4 < x \leq 8$ m) would present very similar results ideally, as the room can be considered symmetrical. However, in a real scenario there might be some variations due to the effect of non-ideal diffuse reflections from the walls, which were not considered in this work [17].

External interferences from daylight (which had much lower amplitude than the artificial light inside the room) and from other transmitters were mitigated by the techniques applied for light modulation and optical measurements. The idea was to modulate a pulsed signal in a short period of time with a known shape and two light levels: OFF (LED turned off) and ON (maximum light intensity). This signal was modulated in one transmitter at a time, while all the other were kept in ON level, avoiding unwanted flickering in the room. In the receiver side the signal was sampled, both levels were averaged and subtracted from each other so that the amplitude of the pulses could be measured individually and the effect of the day light and interference from other transmitters could be eliminated. This concept is shown in Fig. 9.

Another important information is that only the light fixtures connected to transmitters were used and the remaining light fixtures connected to the standard current-controlled power supplies were turned off during the tests.

After the calculation of the positioning errors for every point p inside the semi-plane P with $z = 0.85$ m, the 2D error plane was plotted in Fig. 10 and the 3D error plane in Fig. 11. The only difference between them is that the z component of the error is considered for the 3D, while it is not considered for 2D. And for both graphs it is possible to observe that the error is higher in the edges and especially in the corners of the room.

These figures give an accurate idea of the error plane along with the room, while Figure 12 shows the semi-plane P inside the room area and the exact position of the light fixtures.

Following, the average and standard deviation of the 2D and 3D error measurements are presented respectively by Tab. 1 and Tab. 2 with four different constraints. In both tables the structure is similar, the first line represents the

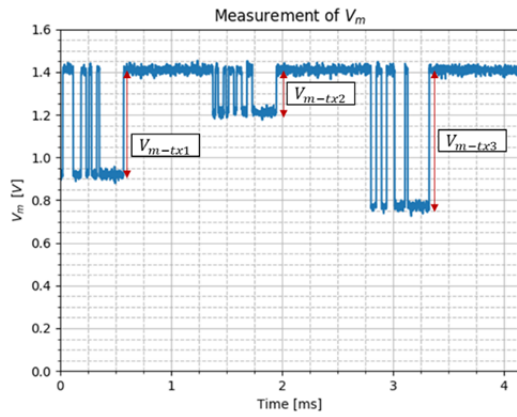


Fig. 9. Measurement of V_m from transmitters tx1, tx2 and tx3.

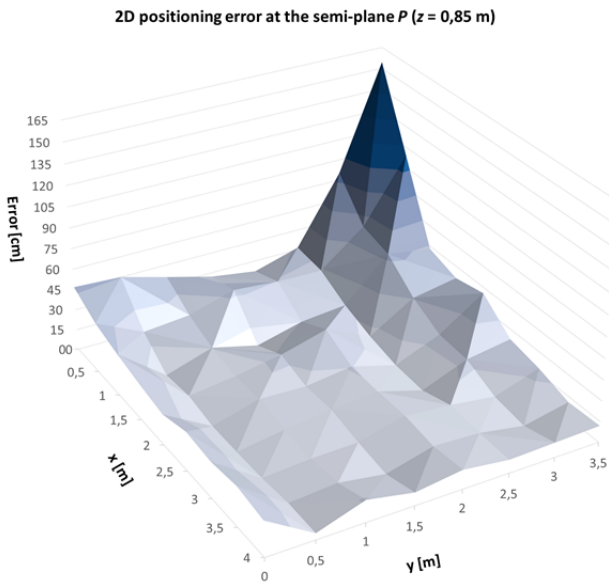


Fig. 10. Absolute value of the 2D positioning error at the semi-plane P with height $z = 0.85$ m.

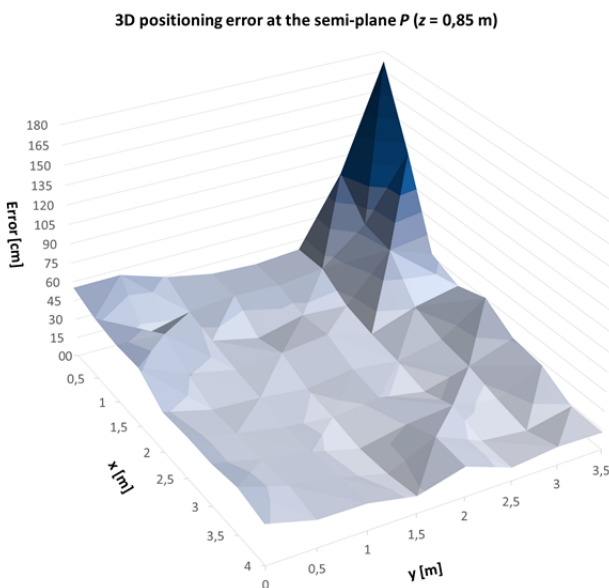


Fig. 11. Absolute value of the 3D positioning error at the semi-plane P with height $z = 0.85$ m.

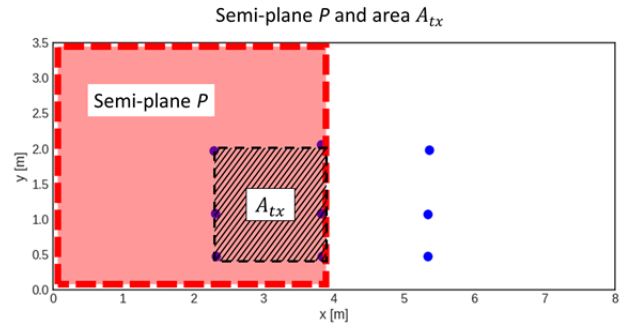


Fig. 12. Top view of the semi-plane P and area A_{tx} , where the positions of the light fixtures connected to transmitters are represented by blue dots.

2D error	μ [cm]	σ [cm]
At any position	22.6309639	22.8296232
$d_{wall} \geq 80$ cm	11.6294646	4.75989936
Inside A_{tx}	12.4215197	8.4426113
$d_{wall} \geq 50$ cm, inside A_{tx}	8.70025085	4.39585211

Tab. 1. Mean and standard deviation of the 2D error.

3D error	μ [cm]	σ [cm]
At any position	31.3036092	24.2681113
$d_{wall} \geq 80$ cm	18.2487085	5.85954397
Inside A_{tx}	21.1677697	7.802871054
$d_{wall} \geq 50$ cm, inside A_{tx}	18.1285318	4.95921642

Tab. 2. Mean and standard deviation of the 3D error.

average and standard deviation for all the error measurements performed in the semi-plane P ; in the second just the measurements at least 80 cm far from the closest wall were considered; in the third just the measurements inside the area below the light fixtures connected to transmitters (A_{tx}) shown in Fig. 12; and the last line deals with the measurements inside the same area A_{tx} , but excludes those closer than 50 cm to the closest wall.

5. Discussion

One of the most straightforward and important outcomes from the figures presented in Sec. 4 is that the positioning error for both 2D and 3D is higher in the regions closer to the walls and specially in the regions closer to the corners. It might be explained by the fact that the walls of the room are a source of reflection and close to those regions the accuracy of the distance measurements is degraded, causing higher positioning errors.

After these observations, it was evident that the proximity of the walls plays an important role in the accuracy of the results output by the indoor positioning system. In order to have a deeper understanding of this relation, it is opportune to plot the positioning error versus the distance of the closest wall.

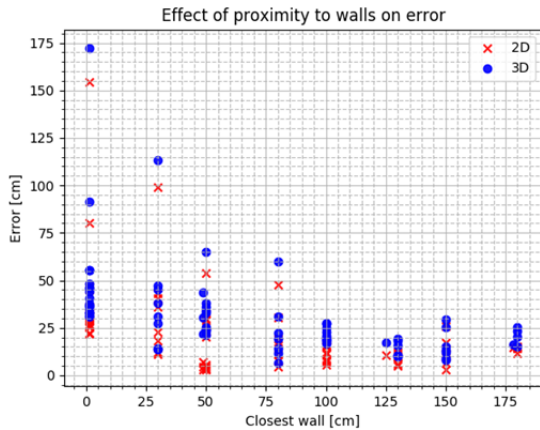


Fig. 13. Effect of the proximity of walls on 2D and 3D error.

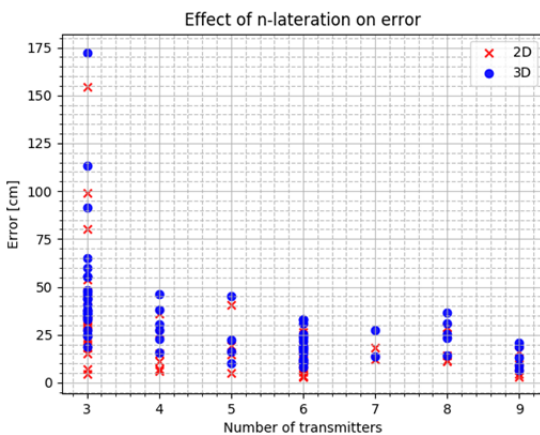


Fig. 14. Effect of n-lation on 2D and 3D error.

Observing Fig. 13 it is evident that measurements performed close to walls present a higher variance of error. In addition, in the special case where the receiver is touching the walls, all the error values are above the corresponding 2D or 3D average error module at any position presented by Tab. 1 and Tab. 2. However, in spite of this connection, no linear, quadratic or exponential curve could be fitted in the graph with $R^2 > 0.5$ meaning that the relation of the distance of the closest wall on the error measurement might be very complex and/or dependent on other additional factors.

Following this investigation, it was also convenient to understand the correlation of the positioning error with the number of transmitters used for the multilateration (N) in each measurement. This data is also somehow related to the distance between the transmitters and the receiver because in this case if the transmitters are not detected it usually means that they are distant from the receiver in a way that it would be out of its amplification range.

Observing Fig. 14 it is clear that multilaterations performed with more transmitters tend to have lower absolute error values and lower variance. Another important fact is that with trilateration (when only three transmitters are used) the positioning error variance is higher than with multilateration for any number of N . This statement is reinforced by the fact that all 2D and 3D errors with a magnitude above 50 cm were registered for $N = 3$.

6. Conclusion

In this work, a method for real-time indoor positioning based on multilateration using the RSS provided by VLC was presented and deployed. In the proposed system, the directivity of the light fixtures was corrected by a procedure described in Sec. 3.1. Further, in Sec. 3.2, a dynamic method to perform multilateration with as much transmitters as possible for improved accuracy was described. Finally, in Sec. 4 it was explained how the measurements mitigated the interference from daylight. In Sec. 4 it was also shown that less than 10 cm average 2D error was achieved in the best-case scenario while the average 2D error at any position inside the test room was lower than 25 cm.

It was evident that the positioning error module might depend on several variables. Section 5 presented some relations between the error and two of them: First, the distance between the closest walls and the mobile device and second, the distance between transmitters and receiver and number of transmitters used in the multilateration.

The effect of the distance between the walls and the mobile device on the error measurements might be explained by the reflections of the walls. In other words, the closer the receiver is from any of the walls, the higher is the effect of reflected light from that wall in the position estimation.

Following, the effect of the distance between the transmitters and receiver on the positioning error could be explained mainly by three reasons. Firstly, if $R_t(\varphi)$ was not perfectly estimated the higher d is, the higher is the error. Secondly, the closer the receivers are to the transmitters, the higher is the number of transmitters used in multilateration, minimizing errors generated by one or few erroneous distance measurements. And thirdly, if the transmitters are more distant to the receiver the value of V_m will be smaller and closer to the noise floor of the receiver, this way decreasing the signal to noise ratio, what impacts negatively on the accuracy of the measurements.

Further on, the imprecision of the measurements could also be explained by several variables that were not measured or were not considered, such as variation in the dimensions of the light fixtures, variation of P_t for each LED, errors in the definition of the transmitters' coordinates, errors in the measurement of $(x_{\text{real}}, y_{\text{real}}, z_{\text{real}})$, A_{eff} not being a constant and depending on the receiving angle ψ and so on.

Regardless of which are the sources of error, the average 2D error magnitude achieved inside A_{tx} with $d_{\text{wall}} \geq 50$ cm was 8.7 cm while the overall average was 22.63 cm. It means a similar system could be used for indoor positioning in places where relatively high accuracy is needed, outstanding technologies such as GPS for indoor environments [2].

These statements are reinforced by the fact that with a VLC IPS the same source of light might be used for illumination, communication, and positioning. In the particular

case of the system proposed by this work, it was possible to achieve a luminous efficacy of 75.8 lm/W. This is advantageous because it might lead to reduced operational costs as the energy spent will be shared among illumination, positioning, and communication and to reduce installation costs as only one infrastructure would be required for all these three purposes.

Acknowledgments

This research had a joint cooperation between Furukawa Electric LatAm (FEL), Furukawa Electric Institute of Technology (FETI) and the research of Dr. Eszter Udvary which was supported by the BME NC TKP2020 grant of NKFIH Hungary.

References

- [1] SAND, S., DAMMANN, A., MENSING, C. *Positioning in Wireless Communications Systems*. 1st ed. Chichester (UK): Wiley, 2014. ISBN: 978-0-4707-7064-1
- [2] ZANDBERGEN, P. A., BARBEAU, S. J. Positional accuracy of assisted GPS data from high-sensitivity GPS-enabled mobile phones. *The Journal of Navigation*, 2011, vol. 64, no. 3, p. 381–399. DOI: 10.1017/S0373463311000051
- [3] LUO, J., FAN, L., LI, H. Indoor positioning systems based on visible light communication: State of the art. *IEEE Communications Surveys & Tutorials*, 2017, vol. 19, no. 4, p. 2871–2893. DOI: 10.1109/COMST.2017.2743228
- [4] HASSAN, N. U., NAEEM, A., PASHA, M. A., et al. Indoor positioning using visible led lights: A survey. *ACM Computing Surveys*, 2015, vol. 48, no. 2, p. 1–32. DOI: 10.1145/2835376
- [5] WANG, W., HUANG, J., CAI, S., et al. Design and implementation of synchronization-free TDOA localization system based on UWB. *Radioengineering*, 2019, vol. 28, no. 1, p. 320–330. DOI: 10.13164/re.2019.0320
- [6] KARASEK, R., VEJRAZKA, F. The DVB-T-based positioning system and single frequency network offset estimation. *Radioengineering*, 2018, vol. 27, no. 4, p. 1155–1165. DOI: 10.13164/re.2018.1155
- [7] GHASSEMLOOY, Z., ALVES, L. N., ZVANOVEC, S., et al. *Visible Light Communications: Theory and Applications*. 1st ed. New York (USA): CRC Press, 2017. ISBN: 978-1-4987-6753-8
- [8] KHAN, L. U. Visible light communication: Applications, architecture, standardization, and research challenges. *Digital Communications and Networks*, 2017, vol. 3, no. 2, p. 78–88. DOI: 10.1016/j.dcan.2016.07.004
- [9] UYSAL, M., CAPSONI, C., GHASSEMLOOY, Z., et al. (Eds.) *Optical Wireless Communications: An Emerging Technology*. 1st ed. Switzerland: Springer, 2016. ISBN: 978-3-319-30200-3
- [10] LUO, P., ZHANG, M., ZHANG, X., et al. An indoor visible light communication positioning system using dual-tone multi-frequency technique. In *The 2nd International Workshop on Optical Wireless Communications (IWOW)*. Newcastle upon Tyne (UK), 2013, p. 25–29. DOI: 10.1109/iwow.2013.6777770
- [11] KUO, Y. S., PANNUTO, P., HSIAO, K. J., et al. Luxapose: Indoor positioning with mobile phones and visible light. In *Proceedings of the 20th Annual International Conference on Mobile Computing and Networking (MobiCom)*. ACM Press (USA), 2014, p. 447–458. DOI: 10.1145/2639108.2639109
- [12] DO, T.-H., YOO, M. TDOA-based indoor positioning using visible light. *Photonic Network Communication*, 2014, vol. 27, no. 2, p. 80–88. DOI: 10.1007/s11107-014-0428-4
- [13] YANG, Z., WANG, Z., ZHANG, J., et al. Wearables can afford: Light-weight indoor positioning with visible light. In *Proceedings of the 13th Annual International Conference on Mobile Systems*. Florence (Italy), 2015, p. 317–330. DOI: 10.1145/2742647.2745924
- [14] KIM, H., KIM, D., YANG, S., et al. An indoor visible light communication positioning system using a RF carrier allocation technique. *Journal of Lightwave Technology*, 2011, vol. 31, no. 1, p. 134–144. DOI: 10.1109/jlt.2012.2225826
- [15] KAHN, J. M., BARRY, J. R. Wireless infrared communications. *Proceedings of IEEE*, 1997, vol. 85, no. 2, p. 265–298. DOI: 10.1109/5.554222
- [16] MOHAIMENUR RAHMAN, A. B. M., LI, T., WANG, Y. Recent advances in indoor localization via visible lights: A survey. *Sensors*, 2020, vol. 20, no. 5, p. 1–26. DOI: 10.3390/s20051382
- [17] VITASEK, J., KOUDELKA, P., LATAL, J., et al. Indoor optical free space networks – Reflectivity of light on building materials. *Przeglad Elektrotechniczny*, 2011, vol. 87, p. 41–44. ISSN: 0033-2097

About the Authors...

Marcos S. P. dos S. LIMA JUNIOR was born in Curitiba, Brazil in 1990. In 2013 he received his B.Sc. in Industrial Electrical Engineering - Automation from the Federal University of Technology - Paraná (UTFPR), Brazil. In 2019 he received his M.Sc. in Electrical Engineering from Budapest University of Technology and Economics (BME), Hungary. Since 2014 he has been working for Furukawa Electric LatAm in telecommunications R&D. His current research interests are in the field of Visible Light Communications and Indoor Positioning Systems.

Miklos Peter HALAPI was born in Budapest, Hungary in 1990. He received his M.Sc. in Industrial Product Design from the Budapest University of Technology and Economics (BME), Budapest, Hungary, in 2014. He is currently a product development engineer at Furukawa Electric Institute of Technology. His main field of interest is design and optimization of industrial and home lighting systems concerning the optical output of the system and production design, such as thermoforming studies and rapid prototyping.

Eszter UDVARY received the Ph.D. degree in Electrical Engineering from the Budapest University of Technology and Economics (BME), Budapest, Hungary, in 2009. She is currently an Associate Professor at BME, Dept. of Broadband Info-communications and Electromagnetic Theory, where she leads the Optical and Microwave Telecommunication Lab. Dr. Udvary's research interests are in the broad areas of optical communications, include optical and microwave communication systems, radio over fiber systems, optical and microwave interactions and applications of special electro-optical devices.